Curvature and Temperature Discrimination Using Multimode Interference Fiber Optic Structures—A Proof of Concept

Susana Silva, Edwin G. P. Pachon, Marcos A. R. Franco, Pedro Jorge, J. L. Santos, F. Xavier Malcata, Cristiano M. B. Cordeiro, and Orlando Frazão

***Abstract*—Singlemode-multimode-singlemode fiber structures (SMS) based on distinct sections of a pure silica multimode fiber (coreless-MMF) with diameters of 125 and 55 μm, were reported for the measurement of curvature and temperature. The sensing concept relies on the multimode interference that occurs in the coreless-MMF section and, in accordance with the length of the MMF section used, two fiber devices were developed: one based on a bandpass filter (self-image effect) and the other on a band-rejection filter. Maximum sensitivities of 64.7 nm·m and 13.08 pm/°C could be attained, for curvature and temperature, respectively, using the band-rejection filter with 55 μm-MMF diameter. A proof of concept was also explored for the simultaneous measurement of curvature and temperature by means of the matrix method.**

***Index Terms*—Curvature, multimode interference, optical fiber sensors, SMS fiber structure, self-imaging, simultaneous measurement, temperature.**

I. Introduction

MULTIMODE INTERFERENCE (MMI) is a well-established concept in integrated optics and recently in optical fibers [1], [2]. MMI-based fiber devices have been explored for several applications using either the self-imaging phenomena or the band-rejection filtering [2], [3]. MMI devices usually rely on a singlemode-multimode-singlemode (SMS) fiber configuration where a step-index multimode fiber (MMF) is used. To obtain a bandpass filter, a specific MMF length corresponding to the self-imaging phenomena is required [1]. In other hand, a band-rejection filter is achieved in the operation wavelength of 1550 nm with ca. 40 mm-long MMF section [2]. Recently, it was demonstrated that controlling the process of the taper fabrication in the MMF region it is possible to attain a bandpass filter in the desired operation wavelength [4].

MMI fiber devices have been developed mainly for fiber laser applications [5] or sensing elements like strain [6], temperature [7], curvature [8], refractive index [9] and simultaneous measurement of strain and temperature [10], [11]. Recently, a curvature SMS sensor with residual sensitivity to temperature and strain was also proposed [12].

This work presents a detailed study of SMS fiber structures based on a coreless-MMF for the simultaneous measurement of curvature and temperature. Two different fiber structures were developed as bandpass filter (self-image concept) and band-rejection filter. Also, MMFs with 125 and 55 μm diameter were used for each device. Finally, a matrix equation is proposed for simultaneous measurement of the physical parameters analyzed.

II. Experimental Results

The sensing head consists of a SMS fiber structure, i.e., a coreless-MMF section (pure silica rod) spliced between two SMFs and interrogated in transmission, as it is schematically shown in Fig. 1. A broadband source (BBS) in the 1550 nm spectral range and 300 nm bandwidth was used, and an optical spectrum analyzer (OSA) as the interrogation unit. The principle underlying the SMS fiber structure concept is based on the premise that when the light field coming from the input SMF enters the coreless-MMF, interference between the different modes occurs along the MMF section.

The light is coupled into the output SMF—and it will depend on the amplitudes and relative phases of the several modes at the exit end of the coreless-MMF. Therefore, the coupling efficiency, for a given length L of the MMF section, is strongly wavelength-dependent. In this work, the operating mechanism of the sensing head relies on either constructive or destructive interference at the output end of the coreless-MMF section, which occurs for a specific length of the MMF used. The result is a bandpass (BP) or a band-rejection (BR) filter with unique spectral characteristics that, in principle, will have different

Manuscript received June 20, 2012; revised August 31, 2012; accepted September 30, 2012. Date of publication October 05, 2012; date of current version December 05, 2012. This work was supported in part by a bi-national collaboration project, CAPES-FCT Brazil/Portugal (# 293/11, coordinated by authors C. M. B. Cordeiro and P. Jorge), in part by FINEP, in part by project Pró-Defesa CAPES/Ministério da Defesa (ref. 23038.029912/2008-05), and in part by project MICROPHYTE (ref. PTDC/EBB-EBI/102728/2008), funded by EU and the Portuguese State and coordinated by author F. X. Malcata. The work of S. Silva was supported in part by a Ph.D. fellowship (ref. SFRH/BD/47799/2008), also funded by EU and the Portuguese State and supervised by author F. X. Malcata.

S. Silva, P. Jorge, J. L. Santos and O. Frazão are with INESC Porto and Departamento de Física e Astronomia da Faculdade de Ciências da Universidade do Porto, Rua do Campo Alegre 687, 4169-007 Porto, Portugal (e-mail: sfsilva@inescporto.pt).

E. G. P. Pachon and C. M. B. Cordeiro are with Instituto de Física "Gleb Wataghin," Universidade Estadual de Campinas—UNICAMP, 13085-859 Campina , São Paulo, Brazil.

M. A. R. Franco is with Instituto de Estudos Avançados, São José dos Campos-São Paulo 12237-970, Brazil.

F. X. Malcata is with Instituto Superior da Maia (ISMAI), Avenida Carlos Oliveira Campos, 4475-690 Avioso S. Pedro, Portugal, and also with ITQB—Instituto de Tecnologia Química e Biológica, Universidade Nova de Lisboa, Avenida da República, 2780-157 Oeiras, Portugal (e-mail: fmalcata@ismai.pt).

Color versions of one or more of the figures in this paper are available online at http://ieeexplore.ieee.org.

Digital Object Identifier 10.1109/JLT.2012.2222865

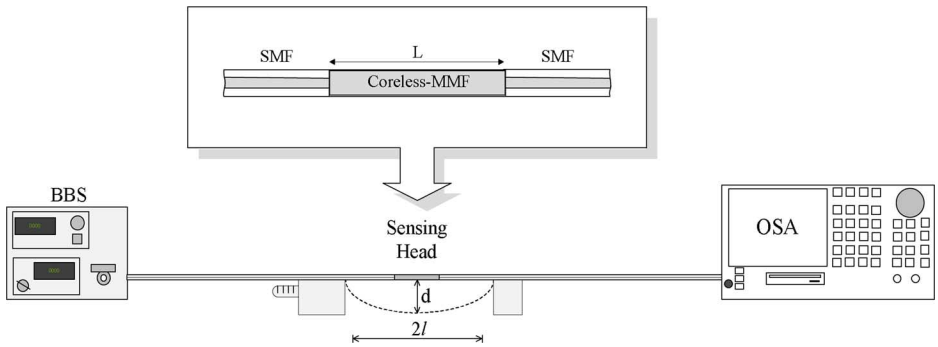

Fig. 1. Experimental setup and detail of the coreless-MMF based-SMS fiber structure.

TABLE I
OPTIMIZED LENGTH OF THE CORELESS-MMF SECTIONS

	Coreless-MMF length (mm)	
	Bandpass filter	Band-rejection filter
SMS_{125}	58.23	14
SMS_{55}	11.45	26.4

sensitivities to curvature. For each sensing device, two coreless-MMFs with different diameters were used, namely 125 and 55 μm (SMS_{125} and SMS_{55}, respectively). Splices between the SMF and the 55 μm-coreless-MMF were performed manually with a fiber fusion splicing machine. Due to the smaller diameter of this fiber, perfect alignment in the splicing process could not be guaranteed; a maximum misalignment of $\sim$5 μm for SMS_{55} was estimated. When the 125 μm-coreless-MMF was used, automatic splice could be performed (SM-MM program). The length of each coreless-MMF section was set in order to provide a bandpass or a band-rejection peak in the operation wavelength range of 1400–1700 nm. The optimized length found, for each coreless-MMF section of each sensing head, is summarized in Table I as follows:

In the case of the bandpass filter based-sensors, the first self-image length was selected for experimental analysis. Previous studies have shown that the first self-image (and multiples) exhibits minimum losses and therefore maximum amplitudes of the spectral signals may be achieved [3]–[9].

Taking the case of the bandpass filter (self-imaging effect), a 3D-simulation based on the BPM method [13] was used to investigate the beam behavior in the coreless-MMF section of an SMS fiber structure in transmission. The modeling of light propagation was done for a pure silica rod with a refractive index (RI) of 1.444, external RI of 1.0, and two different diameters, viz. 55 and 125 μm. SMFs with core and cladding diameters of 8.2 and 125 μm, respectively, were used for both light input and output of the coreless-MMF section. All fibers were aligned along the same axis and possessed a circular cross-section. The number of propagating modes in each MMF was also estimated [14]: values of $\sim$7000 and $\sim$35000 were found for the 55 and 125 μm-diameter coreless-MMFs, respectively. The intensity distribution of the electric field on the xz plane at

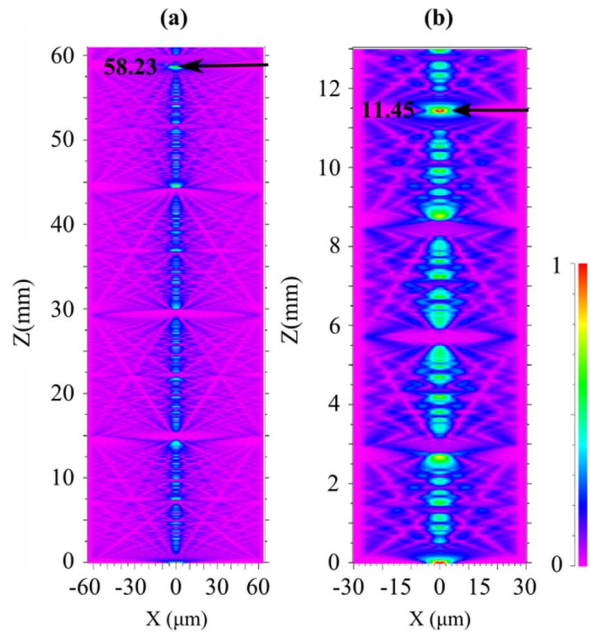

Fig. 2. Intensity distribution of the electric field on the xz plane at 1550 nm-wavelength, for the bandpass filters with (a) 125 μm and (b) 55 μm coreless-MMF diameters.

1550 nm-wavelength, for the simulated bandpass filters with diameters of 55 and 125 μm are plotted in Fig. 2(a) and (b), respectively.

The numerical simulations have shown that the optimized MMF length was 11.5 and 58.9 mm, for the fiber structures with coreless-MMF diameters of 55 and 125 μm, respectively, which is in agreement with the experimental values presented in Table I.

A. Bandpass Filter Based-SMS Fiber Sensor

Bandpass filtering arises from the self-imaging effect which occurs when the light field at the input of the coreless-MMF section is replicated on its output, in both amplitude and phase, for a specific wavelength. At the exit end of the coreless-MMF, all the light field condensates into one point, due to constructive interference between the several modes, to be recoupled into the output SMF, and thus providing a well defined bandpass wavelength peak. Fig. 3 presents the first self-image spectral response

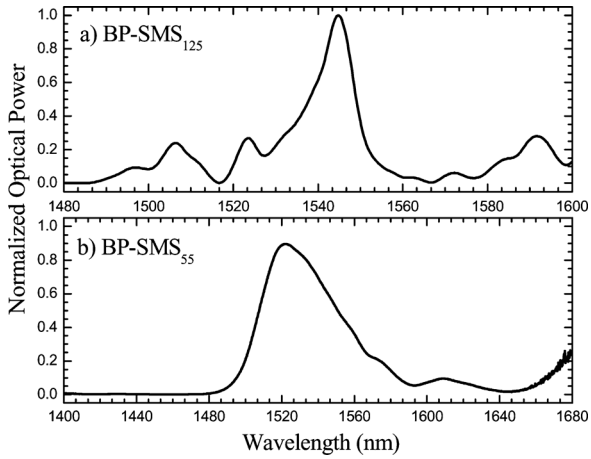

Fig. 3. Spectral responses of the bandpass filters with coreless-MMF diameters of (a) 125 and (b) 55 μm (BP$-$SMS$_{125}$ and BP$-$SMS$_{55}$, respectively).

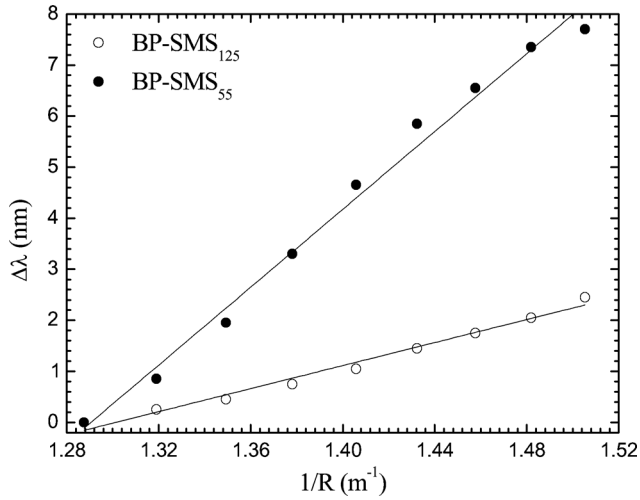

Fig. 4. Curvature response of the bandpass filters, (○) BP$-$SMS$_{125}$ and (●) BP$-$SMS$_{55}$.

of the bandpass filters with coreless-MMF diameters of a) 125 and b) 55 μm (BP$-$SMS$_{125}$ and BP$-$SMS$_{55}$, respectively).

The sensing structures, BP$-$SMS$_{125}$ and BP$-$SMS$_{55}$, have a wavelength peak centered at 1544.8 and 1522.4 nm, respectively. The behavior of each resonance when subjected to curvature was characterized by fixing each SMS fiber structure at two points, 250 mm distanced from each other; one of these points is a translation stage that allows the fiber to bend (see Fig. 1). The bending displacement, d, was applied to each SMS via sequential 40 μm-displacements.

Hence, the curvature $(1/R)$ of the fiber structure changed by $2d/(d^2 + l^2)$, where l is the half distance between the two fixed points. The obtained results are depicted in Fig. 4. Results show that both sensors have linear responses in the curvature range studied (1.28-1.52) m^{-1}. Also, sensitivities to curvature of (11.3 ± 0.2) nm·m and (38.1 ± 0.7) nm·m, for BP$-$SMS$_{125}$ and BP$-$SMS$_{55}$, respectively, could be achieved. Typically, the field profile of an SMS fiber structure is symmetrically distributed along the direction of propagation of the coreless-MMF. Although, when curvature is applied, this symmetry is broken. Fig. 5 shows an example of the loss of symmetry when curvature is applied to BP$-$SMS$_{55}$.

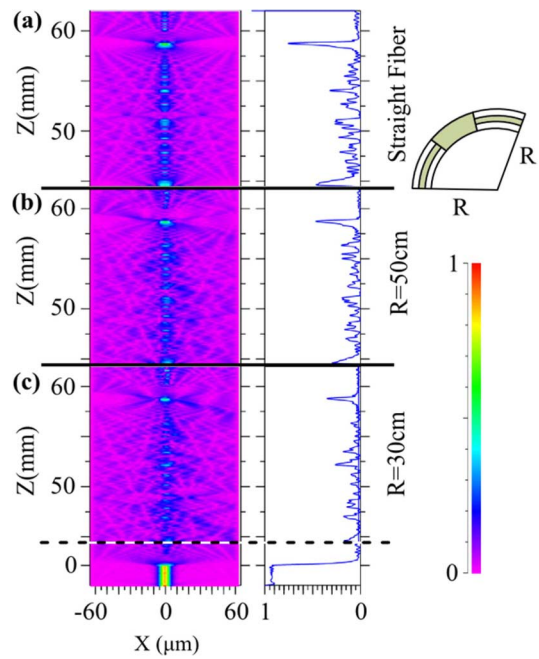

Fig. 5. Intensity distribution of the BP-SMS$_{55}$ electric field on the xz plane at 1550 nm-wavelength, and for different curvatures applied: (a) straight fiber, (b) R = 50 cm and (c) R = 30 cm.

B. Band-Rejection Filter Based-SMS Fiber Sensor

Multimode interference characterizes by the field profile variation along the MMF section, although remaining symmetrically distributed along the direction of propagation.

The band-rejection filter appears in a specific operation wavelength when interference between specific modes is destructive in the core region. This effect may be observed with different lengths of the coreless-MMF. The result is the amplitude decrease of the spectral signal in such way that a band-rejection based-spectral response is observed. Fig. 6 shows the optical spectra of the band-rejection filters with coreless-MMF diameters of a) 125 and b) 55 μm (BR$-$SMS$_{125}$ and BR$-$SMS$_{55}$, respectively).

Each sensing structure presents a wavelength band-rejection centered at 1540.2 and 1576.7 nm, for BR$-$SMS$_{125}$ and BR$-$SMS$_{55}$, respectively. These fiber structures were also characterized in terms of curvature. Each sensing device was fixed at two points, 250 mm distanced from each other. The bending displacement, d, was applied by means of the translation stage via sequential 25 μm-displacements. The sensitivities to curvature are presented in Fig. 7.

One can observe that both sensors have linear responses in the curvature range studied (1.28–1.52) m^{-1}, and sensitivities of (-12.1 ± 0.1) nm·m and (-64.7 ± 0.5) nm·m, for BR$-$SMS$_{125}$ and BR$-$SMS$_{55}$, respectively, could be attained. Table II summarizes the attained results.

Similar to the bandpass filter, interference between higher-order modes is more affected by bending of the MMF section, while lower-order modes are focused within a smaller area near

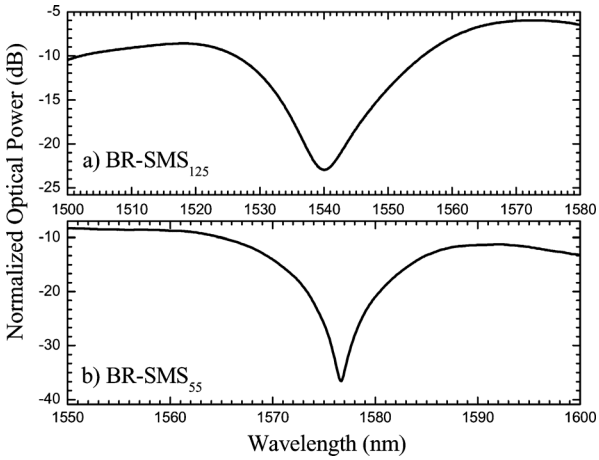

Fig. 6. Spectral responses of the band-rejection filters with coreless-MMF diameters of (a) 125 and (b) 55 μm (BR−SMS$_{125}$ and BR−SMS$_{55}$, respectively).

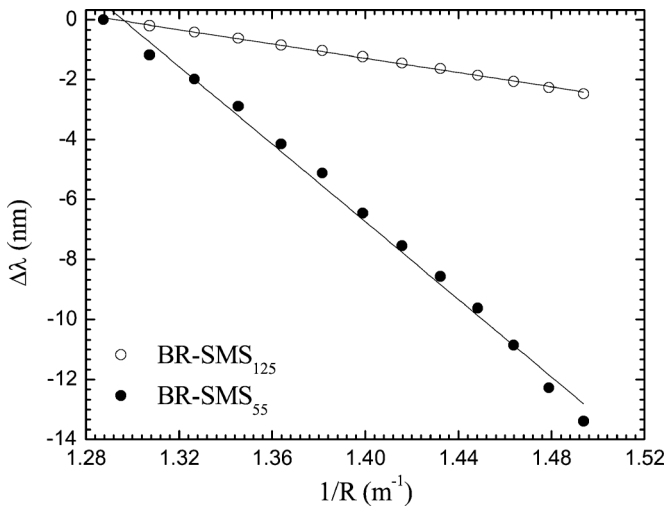

Fig. 7. Curvature response of the band-rejection filters, (○) BR−SMS$_{125}$ and (●) BR−SMS$_{55}$.

TABLE II
CURVATURE SENSITIVITIES OF THE SMS FIBER STRUCTURES

	Sensitivity to curvature (nm.m)	
	Bandpass filter	Band-rejection filter
SMS$_{125}$	11.3	-12.1
SMS$_{55}$	38.1	-64.7

the fiber core and are consequently less affected by the bending disturbance. Therefore, both filter types will present sensitivity increase to curvature with the decrease of the coreless-MMF diameter.

C. Temperature Measurement

The response of the BP- and BR-SMS sensing heads to temperature variations was also characterized, as shown in Figs. 8 and 9, respectively. Each structure was placed in a tube furnace, and submitted to increasing values of temperature in the range 0–80°C, with 5°C steps.

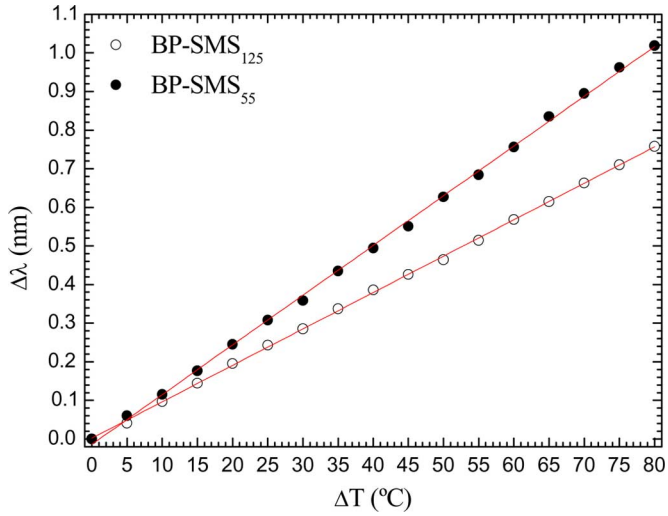

Fig. 8. Wavelength shift versus temperature variation for the bandpass filter.

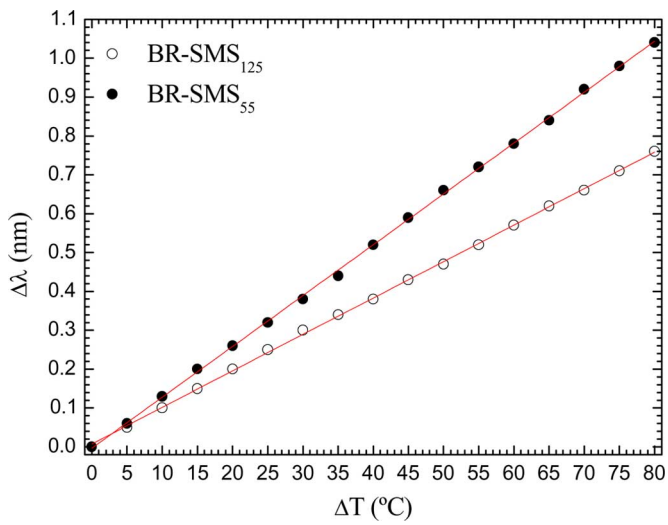

Fig. 9. Wavelength shift versus temperature variation for the band-rejection filter.

TABLE III
TEMPERATURE SENSITIVITIES OF THE SMS FIBER STRUCTURES

	Sensitivity to temperature (pm/ºC)	
	Bandpass filter	Band-rejection filter
SMS$_{125}$	9.44	9.38
SMS$_{55}$	12.88	13.08

The SMS fiber-based filters with the same diameter have similar sensitivities to temperature. This was somewhat expected since the temperature variation does not change the SMF-silica rod launching conditions; the results are determined by the temperature dependence of the refractive index and the thermal expansion of the silica fiber material. In both cases, one can observe that the sensing structures with a 55 μm-coreless-MMF are more sensitive to temperature; this happens because the multimode interference is more affected by the thermal expansion in the MMF with a smaller diameter. Table III summarizes the temperature sensitivity values attained for the SMS fiber structures.

TABLE IV
MATRIX EQUATIONS GIVEN BY THE COMBINATION OF BR AND BP-SMS FIBER STRUCTURES

		BP-SMS	
		55 μm	125 μm
BR-SMS	55 μm	$\begin{bmatrix}\Delta T\\ \Delta C\end{bmatrix}=\frac{1}{D}\begin{bmatrix}\kappa_{C(BR-SMS_{55})} & -\kappa_{C(BP-SMS_{55})}\\ -\kappa_{T(BR-SMS_{55})} & \kappa_{T(BP-SMS_{55})}\end{bmatrix}\begin{bmatrix}\Delta\lambda_{BP-SMS_{55}}\\ \Delta\lambda_{BR-SMS_{55}}\end{bmatrix}$	$\begin{bmatrix}\Delta T\\ \Delta C\end{bmatrix}=\frac{1}{D}\begin{bmatrix}\kappa_{C(BR-SMS_{55})} & -\kappa_{C(BP-SMS_{125})}\\ -\kappa_{T(BR-SMS_{55})} & \kappa_{T(BP-SMS_{125})}\end{bmatrix}\begin{bmatrix}\Delta\lambda_{BP-SMS_{125}}\\ \Delta\lambda_{BR-SMS_{55}}\end{bmatrix}$
	125 μm	$\begin{bmatrix}\Delta T\\ \Delta C\end{bmatrix}=\frac{1}{D}\begin{bmatrix}\kappa_{C(BR-SMS_{125})} & -\kappa_{C(BP-SMS_{55})}\\ -\kappa_{T(BR-SMS_{125})} & \kappa_{T(BP-SMS_{55})}\end{bmatrix}\begin{bmatrix}\Delta\lambda_{BP-SMS_{55}}\\ \Delta\lambda_{BR-SMS_{125}}\end{bmatrix}$	$\begin{bmatrix}\Delta T\\ \Delta C\end{bmatrix}=\frac{1}{D}\begin{bmatrix}\kappa_{C(BR-SMS_{125})} & -\kappa_{C(BP-SMS_{125})}\\ -\kappa_{T(BR-SMS_{125})} & \kappa_{T(BP-SMS_{125})}\end{bmatrix}\begin{bmatrix}\Delta\lambda_{BP-SMS_{125}}\\ \Delta\lambda_{BR-SMS_{125}}\end{bmatrix}$

TABLE V
MATRIX EQUATIONS WITH THE OBTAINED CURVATURE AND TEMPERATURE COEFFICIENTS, AND GIVEN BY THE COMBINATION OF BR AND BP-SMS FIBER STRUCTURES

		BP-SMS	
		55 μm	125 μm
BR-SMS	55 μm	$\begin{bmatrix}\Delta T\\ \Delta C\end{bmatrix}=\frac{1}{D}\begin{bmatrix}-64.7 & -38.1\\ -13.08\times10^{-3} & 12.88\times10^{-3}\end{bmatrix}\begin{bmatrix}\Delta\lambda_{BP-SMS_{55}}\\ \Delta\lambda_{BR-SMS_{55}}\end{bmatrix}$	$\begin{bmatrix}\Delta T\\ \Delta C\end{bmatrix}=\frac{1}{D}\begin{bmatrix}-64.7 & -11.3\\ -13.08\times10^{-3} & 9.44\times10^{-3}\end{bmatrix}\begin{bmatrix}\Delta\lambda_{BP-SMS_{125}}\\ \Delta\lambda_{BR-SMS_{55}}\end{bmatrix}$
	125 μm	$\begin{bmatrix}\Delta T\\ \Delta C\end{bmatrix}=\frac{1}{D}\begin{bmatrix}-12.1 & -38.1\\ -9.38\times10^{-3} & 12.88\times10^{-3}\end{bmatrix}\begin{bmatrix}\Delta\lambda_{BP-SMS_{55}}\\ \Delta\lambda_{BR-SMS_{125}}\end{bmatrix}$	$\begin{bmatrix}\Delta T\\ \Delta C\end{bmatrix}=\frac{1}{D}\begin{bmatrix}-12.1 & -11.3\\ -9.38\times10^{-3} & 9.44\times10^{-3}\end{bmatrix}\begin{bmatrix}\Delta\lambda_{BP-SMS_{125}}\\ \Delta\lambda_{BR-SMS_{125}}\end{bmatrix}$

D. Concept for Simultaneous Measurement of Temperature and Curvature

In this section a proof of concept is explored for the simultaneous measurement of temperature and curvature. The objective is to use the matrix method in order to identify the best pair of SMS fiber sensors able to perform the simultaneous measurement of both physical parameters. The wavelength shifts induced by changes in curvature and temperature are given in the matrix form by:

$$\begin{bmatrix}\Delta\lambda_{i,j}\\ \Delta\lambda_{i,j}\end{bmatrix}=\begin{bmatrix}\kappa_{Ti,j} & \kappa_{Ci,j}\\ \kappa_{Ti,j} & \kappa_{Ci,j}\end{bmatrix}\begin{bmatrix}\Delta T\\ \Delta C\end{bmatrix} \tag{1}$$

The measurand values can be calculated by inverting the matrix (1) as follows:

$$\begin{bmatrix}\Delta T\\ \Delta C\end{bmatrix}=\frac{1}{D}\begin{bmatrix}\kappa_{Ci,j} & -\kappa_{Ci,j}\\ -\kappa_{Ti,j} & \kappa_{Ti,j}\end{bmatrix}\begin{bmatrix}\Delta\lambda_{i,j}\\ \Delta\lambda_{i,j}\end{bmatrix} \tag{2}$$

where $\kappa_{Ci,j}$ and $\kappa_{Ti,j}$ are the curvature and temperature coefficients, $i,j=(\mathrm{BP-SMS}$ or $\mathrm{BR-SMS})$, (55 or 125 μm) and D (nm^2·m/°C) is the matrix determinant. In this case, four matrix solutions are possible as shown in Tables IV and V.

The determinant (D) of each matrix was calculated in order to determine the best solution for simultaneous measurement of curvature and temperature. In order to have a sensing head with proper discrimination performance, the determinant should be as high as possible [15]. The obtained results are presented in Table VI as follows:

TABLE VI
MATRIX DETERMINANTS OBTAINED BY THE COMBINATION OF BR AND BP-SMS FIBER STRUCTURES

		Matrix determinant (nm^2·m/ºC)	
		BP-SMS	
		55 μm	**125 μm**
BR-SMS	**55 μm**	**-1.33**	-0.76
	125 μm	-0.51	-0.22

Therefore, the best value attained (-1.33 nm^2·m/°C) corresponds to the sensing head composed by a $\mathrm{BR-SMS_{55}}$ and $\mathrm{BP-SMS_{55}}$ in series.

III. CONCLUSION

This work presented an SMS fiber structure based on a sections of pure silica MMF for the simultaneous measurement of curvature and temperature as proof concept. Two fiber devices were developed according with the MMF length used: one based on bandpass filtering (self-image effect) and the other on a band-rejection filter. Also, two coreless-MMFs with different diameters were used for each device, viz. 125 and 55 μm, and its influence to curvature and temperature variations was analyzed. Experimental results indicated that the sensing structures using the coreless-MMF with 55 μm diameter had highest sensitivity to both physical parameters. In practice, maximum sensitivities of 38.1 and -64.7 nm·m were attained, for the bandpass $(\mathrm{BP-SMS_{55}})$ and band-rejection $(\mathrm{BR-SMS_{55}})$ fiber devices, respectively. The temperature sensitivity of each SMS

fiber device was also analyzed. The obtained results were explored for simultaneous measurement of temperature and curvature. Using the matrix method it was shown that $\mathrm{BR}-\mathrm{SMS}_{55}$ and $\mathrm{BP}-\mathrm{SMS}5_5$ in series is the best combination for multiparameter measurement.

REFERENCES

[1] L. B. Soldano and E. C. M. Pennings, "Optical multi-mode interference devices based on self-imaging: Principles and applications," *J. Lightw. Technol.*, vol. 13, pp. 615–627, 1995.

[2] O. Frazão, S. Silva, J. Viegas, L. A. Ferreira, F. M. Araújo, and J. L. Santos, "Optical fiber refractometry based on multimode interference," *Appl. Opt.*, vol. 50, pp. E184–188, 2011.

[3] W. S. Mohammed, P. W. E. Smith, and X. Gu, "All-fiber multimode interference bandpass filter," *Opt. Lett.*, vol. 31, pp. 2547–2549, 2006.

[4] C. R. Biazoli, S. Silva, M. A. R. Franco, O. Frazão, and C. M. B. Cordeiro, "Multimode interference tapered fiber refractive index sensors," *Appl. Opt.*, submitted.

[5] A. Castillo-Guzman, J. E. Antonio-Lopez, R. Selvas-Aguilar, D. A. May-Arrioja, J. Estudillo-Ayala, and P. L. Wa, "Widely tunable erbium-doped fiber laser based on multimode interference effect," *Opt. Exp.*, vol. 18, pp. 591–597, 2010.

[6] E. Li, "Sensitivity-enhanced fiber-optic strain sensor based on interference of higher order modes in circular fibers," *IEEE Photon. Technol. Lett.*, vol. 19, pp. 1266–1268, 2007.

[7] R. X. Gao, Q. Wang, F. Zhao, B. Meng, and S. L. Qu, "Optimal design and fabrication of SMS fiber temperature sensor for liquid," *Opt. Commun.*, vol. 283, pp. 3149–3152, 2010.

[8] Y. Gong, T. Zhao, Y. Rao, and Y. Wu, "All-fiber curvature sensor based on multimode interference," *IEEE Photon. Technol. Lett.*, vol. 23, pp. 679–681, 2011.

[9] S. Silva, E. G. P. Pachon, M. A. R. Franco, J. G. Hayashi, F. X. Malcata, O. Frazão, P. Jorge, and C. M. B. Cordeiro, "Ultra-high temperature-sensitivity sensor based on multimode interference," *Appl. Opt.*, vol. 51, pp. 3236–3242, 2012.

[10] Q. Wu, Y. Semenova, A. M. Hatta, P. Wang, and G. Farrell, "Single-mode-multimode-singlemode fiber structures for simultaneous measurement of strain and temperature," *Microw. Opt. Technol. Lett.*, vol. 53, pp. 2181–2185, 2011.

[11] L. Coelho, J. Kobelke, K. Schuster, and O. Frazão, "Multimode interference in outer cladding large-core air-clad photonic crystal fiber," *Microw. Opt. Technol. Lett.*, vol. 54, pp. 1009–1011, 2012.

[12] S. Silva, O. Frazão, J. Viegas, L. A. Ferreira, F. M. Araújo, F. X. Malcata, and J. L. Santos, "Temperature and strain-independent curvature sensor based on a singlemode/multimode fiber optic structure," *Meas. Sci. Technol.*, vol. 22, p. 085201, 2011.

[13] W. Jin, W. C. Michie, G. Thursby, M. Konstantaki, and B. Culshaw, "Simultaneous measurement of strain and temperature: Error analysis," *Opt. Eng.*, vol. 36, pp. 598–609, 1997.

[14] K. Okamoto, *Fundamentals of Optical Waveguides*. New York: Elsevier, 2006.

[15] K. Kawano and T. Kitoh, *Introduction to Optical Waveguide Analysis*. New York: Wiley, 2001, ch. 5, pp. 165–230.

Susana Silva received the degree in applied physics (optics and electronics) and the M.Sc. in optoelectronics and lasers from the University of Porto, Porto, Portugal, in 2004 and 2007, respectively, where she is currently working towards the Ph.D. degree in physics.

She is currently with INESC Porto in the Optoelectronics and Electronic Systems Unit. She has published more than 20 papers in international journals and more than 30 papers in national and international conferences. Her research interests include fiber-optic sensing, Bragg grating technology and biosensing.

Ms. Silva is a member of European Optical Society (EOS).

Edwin G. P. Pachon received the degree in physics (condensed matter) from the Universidad Nacional de Colombia, Bogotá, Colombia in 2010. He is currently working towards the M.Sc. degree in physics at the Universidade Estadual de Campinas, Brazil.

He is currently with IFGW, Departamento de Eletrônica Quântica, in the Laboratório de Fibras Especiais e Materias Fotônicos. His research interest includes fiber-optic sensing.

Marcos A. R. Franco received the B.S. degree in physics from the Pontifical Catholic University, São Paulo, Brazil, in 1983, the M.S. degree in physics from the University of São Paulo, São Paulo, in 1991, and the Ph.D. degree in electrical engineering from the University of São Paulo, in 1999.

He is currently a Researcher at the Institute of Advanced Studies (IEAv), São José dos Campos-SP, and a Professor at the Institute of Technology of Aeronautics (ITA), São José dos Campos-SP, in the postgraduate program in Science and Space Technologies. He is the head of the Computational Electromagnetic Laboratory at IEAv. His main research interests include the applied electromagnetic, computational modeling of electromagnetic devices, optical fibers, fiber optic sensors, photonic crystal fibers, microstructured optical fibers and integrated optics.

Pedro Jorge received the degree in applied physics from the University of Minho, 4710-057 Braga, Portugal, in 1996, the M.Sc. degree in optoelectronics and lasers from the University of Porto, Portugal, in 2000, and in 2006 concluded his Ph.D. program at Porto University in collaboration with the Department of Physics and Optical Sciences at the University of Charlotte, NC.

Since 1997 he has been involved in several research and technology transfer projects related to optical fibre sensing technology, developing new sensing configurations and interrogation techniques for optical sensors, both as a researcher and more recently as project leader and manager. He is currently a Senior researcher at INESC Porto where he leads the Biochemical Sensors team exploring the potential of optical fibre and integrated optics technologies in environmental and medical applications. He has more than 100 publications in the fields of sensors in national and international conferences and peer reviewed journals and also holds two patents.

J. L. Santos received the degree in applied physics (optics and electronics) and the Ph.D. degree in multiplexing and signal processing in fiber-optic sensors from the University of Porto, Porto, Portugal, in 1983 and 1993, and research performed partially at the Department of Physics, University of Canterbury, Kent, U.K.

He is a Full Professor with the Department of Physics, University of Porto, and he was for 15 years the Manager of the Optoelectronics and Electronic Systems Unit, INESC Porto. His main research interests are in the optical fiber sensing field and in optical fiber technology. Dr. Santos is also a member of the Optical Society of America (OSA), The International Society for Optical Engineers (SPIE), and the Planetary Society.

F. Xavier Malcata received the Licenciatura degree in chemical engineering from the University of Porto, Porto, Portugal, in 1988, and the Ph.D. degree in chemical engineering from the University of Wisconsin, Madison, in 1992.

He was Dean of the College of Biotechnology, Portuguese Catholic University, for 11 years, and is currently a Full Professor at the Instituto Superior da Maia, Maia, Portugal. His research interest include various aspects of bioreactor and bioprocess engineering, including analytical devices for monitoring. More recently, the R&D group under his leadership has been investing in microalga-mediated biotechnology, including alternative vectors for production of clean fuels.

Cristiano M. B. Cordeiro received the Ph.D. from the State University of Campinas (UNICAMP), Campinas, Brazil.

He is Assistant Professor with UNICAMP and postdoc from University of Bath, England. Dr. Cordeiro is head of the Specialty Optical Fiber & Photonics Materials Laboratory (LaFE) at UNICAMP. The main research areas of the laboratory are the development and application of silica photonic crystal fibers, microstructured polymer optical fibers and micro/nanofibers. Topics of interest also include the waveguide structural and material post-processing for exploring new fiber functionalities. Applications related with optical devices and sensors, telecommunications and nanophotonics are under investigation.

Orlando Frazão received the degree in physics engineering (optoelectronics and electronics) from the University of Aveiro, Aveiro, Portugal, and the Ph.D. degree in physics from the University of Porto, Porto, Portugal, in 2009.

From 1997 to 1998, he was with the Institute of Telecommunications, Aveiro. Presently, he is a Senior Researcher at the Optoelectronics and Electronic Systems Unit, INESC Porto. He has published about 250 papers, mainly in international journals and conference proceedings, and his present research interests included optical fiber sensors and optical communications.

Dr. Frazão is a member of the Optical Society of America (OSA) and The International Society for Optical Engineers (SPIE).